HHS Public Access

Author manuscript

J Orthop Res. Author manuscript; available in PMC 2021 April 01.

Published in final edited form as:

J Orthop Res. 2020 April ; 38(4): 852–860. doi:10.1002/jor.24512.

Biofilm producing Staphylococcus epidermidis (RP62A strain) inhibits osseous integration without osteolysis and histopathology in a murine septic implant model

Takuya Tomizawa[1], **Masahiro Ishikawa**[1,2], **Sheila N. Bello-Irizarry**[2], **Karen L. de Mesy Bentley**[2,3], **Hiromu Ito**[1], **Stephen L. Kates**[4], **John L. Daiss**[2], **Christopher Beck**[2,5], **Shuichi Matsuda**[1], **Edward M. Schwarz**[2,5], **Kohei Nishitani**[1,2,6]

[1]Department of Orthopaedic Surgery, Graduate School of Medicine, Kyoto University, Kyoto, Japan

[2]Center for Musculoskeletal Research, University of Rochester Medical Center, Rochester, New York, USA.

[3]Pathology and Laboratory Medicine, University of Rochester Medical Center, Rochester, New York, USA.

[4]Department of Orthopaedic Surgery, Virginia Commonwealth University School of Medicine, Richmond, VA, USA.

[5]Department of Orthopedics and Rehabilitation, University of Rochester Medical Center, Rochester, New York, USA

Abstract

Despite its presence in orthopaedic infections, *Staphylococcus epidermidis*'s ability to directly induce inflammation and bone destruction is unknown. Thus, we compared a clinical strain of methicillin-resistant biofilm-producing *Staphylococcus epidermidis* (RP62A) to a highly virulent and osteolytic strain of methicillin-resistant *Staphylococcus aureus* (USA300) in an established murine implant-associated osteomyelitis model. Bacterial burden was assessed by colony forming units (CFUs), tissue damage was assessed by histology and micro-computer tomography (μCT), biofilm was assessed by scanning electron microscopy (SEM), host gene expression was assessed by quantitative polymerase chain reaction (qPCR), and osseous integration was assessed via biomechanical push-out test. While CFUs were recovered from RP62A contaminated implants and surrounding tissues after 14 days, the bacterial burden was significantly less than USA300-infected tibiae ($p<0.001$). Additionally, RP62A failed to produce any of the gross pathologies induced by USA300 (osteolysis, reactive bone-formation, *Staphylococcus* abscess communities, marrow necrosis and biofilm). However, fibrous tissue was present at the implant-host interface, and rigorous SEM confirmed the rare presence of cocci on RP62A-contaminated implants. Gene

[6]To whom correspondence should be addressed, Kohei Nishitani M.D., Ph.D., Department of Orthopaedic Surgery, Graduate School of Medicine, Kyoto University, 54 Shogoin Kawahara Cho, Sakyo, Kyoto, Japan, nkohei@kuhp.kyoto-u.ac.jp | Phone: +81(75) 366-7734.

Authors Contribution

Designed experiments by MI, SNB, SLK, JLD, EMS, and KN, performed experiments by TT, MI, SNB, KLM, and KN, data analysis by TT, MI, SNB, JLD, CB, EMS, KN, writing and editing of manuscript by TT, MI, HI, SLK, JLD, SM, EMS, and KN. All authors have read and approved the final submitted manuscript.

expression studies revealed that IL-1β, IL-6, RANKL, and TLR-2 mRNA levels in RP62A infected bone were increased versus Sterile controls. *Ex vivo* push-out testing showed RP62A infected implants required significantly less force compared to the Sterile group (7.5±3.4 N vs. 17.3±4.1 N; p<0.001), but required 10-fold greater force than USA300 infected implants (0.7±0.3 N; p<0.001). Taken together, these findings demonstrate that *S. epidermidis* is a commensal pathogen whose mechanisms to inhibit osseous integration are limited to minimal biofilm formation on the implant, and low-grade inflammation.

Keywords

implant-associated osteomyelitis; *Staphylococcus epidermidis*; biofilm; loosening

INTRODUCTION

Orthopaedic implant related infections remain a devastating problem that threatens life, wellness and our healthcare systems[1]. *Staphylococci* species are responsible for the majority of implant-associated osteomyelitis, and account for ~80% of cases[1,2]. Historically, *Staphylococci* were distinguished by their ability to produce coagulase; the virulent enzyme which causes fibrin to clot[3]. Examples of this are *S. epidermidis*, which is a representative species of coagulase-negative *Staphylococci* (CNS), and *S. aureus*, which is the most common coagulase-positive organism in implant-associated infection. Clinically, *Staphylococci* strains are further defined by their resistance to methicillin, and the methicillin-resistant *S. aureus* (MRSA) strain USA300 is known to be the most challenging to treat [4]. Previous studies have documented cure rates of 57% from MRSA, 72% from methicillin-sensitive *S. aureus*, and 82% from CNS, at 1 year.[5] In a multicenter, study, the failure rate of treatment for MRSA knee infections was much as 84%.[6] To make matters worse, the emergence of community acquired USA300 strains is a serious problem,[7] as mortality rates from these infections are twice that of trauma and elective orthopaedic wards.[8]

S. epidermidis is a ubiquitous member of the human skin microbiome, and lacks aggressive virulence properties overall. It is also the most common CNS present in implant-associated osteomyelitis, and therefore is considered to be a commensal pathogen[2]. Otto et al. demonstrated the roles of *S. epidermidis* in harmonizing the epithelial microflora.[9] Additionally, Iwase et al. demonstrated that *S. epidermidis* is associated with suppression of *S. aureus*,[10] which suggests a protective role against infection. However, *S. epidermidis* is also considered to be an opportunistic pathogen, as it causes infections in immunocompromised patients with implants.[11] *S. epidermidis* is also present on prosthetic joint infection (PJI),[12] and implants removed for aseptic prosthesis loosening.[13] Interestingly, late-start chronic (low-grade) PJI, which are challenging to diagnose from unspecific clinical signs, false-negative cultures, and low values of serum biomarkers,[14] often contain CNS as the hidden pathogen.[15] Perviously, it has been reported that 8.3% of “aseptic” total joint replacement revisions are actually bacterial culture positive following sonication of the implant, in which CNS was positive in most of these cases.[16] In another report, CNS was detected in 5 out of the 22 cases from patients diagnosed with “aseptic”

loosening or suspicion of uncleanness.[17] It is also reported that biofilms are responsible for 'aseptic' implant-loosening[18].

As described above, although *S. epidermidis* is one of the normal bacterial flora, it also the cause of low grade infection or might be the cause of " aseptic" implant loosening. [9,19] Thus, we aimed to compare and contrast the pathological features of a biofilm-producing strain of methicillin-resistant *Staphylococcus epidermidis* (MRSE) RP62A, which is a strongly adherent, slime-producing, and was originally isolated from a patient with intravascular catheter-associated sepsis.[20] In the RP62A vs. highly virulent USA300 in a quantitative murine model of implant-associated osteomyelitis[21]. We hypothesized that RP62A was less destructive than USA300 but produced a biofilm that inhibits osseous integration of the implant.

Materials and Methods

Staphylococci strains and *in vitro* culture

As a representative of *S. aureus*, USA300 LAC,[22] which is the most prevalent community-acquired MRSA strain, was used. For *Staphylococcus epidermidis,* RP62A, which is biofilm-producing clinical isolate RP62A strain, was used. RP62A is capable of accumulated growth and subsequent biofilm development, which contribute to its pathogenicity in foreign-body infections[20]. All strains were cultured in tryptic soy broth (TSB) media.

Animal surgeries

All animal experiments were performed on the national guidelines under the approval of the university committee on animal resources. The transtibial implant associated osteomyelitis model, which does not display sexual dimorphism, was used as previously described. [21] Briefly, the implant was made of flat stainless-steel wire (cross-section 0.2 mm × 0.5 mm; MicroDyne Technologies, Plainville, CT) which was cut to 4 mm length and bent into an L-shaped implant: long side 3 mm, short side 1 mm. After sterilization, the implant was soaked in the overnight culture of USA300 or RP62A for 20 minutes then air dried for 1 minutes. For control, implant was soaked in broth without bacteria in the same manner. BALB/c female 6–8-week-old mice were anesthetized with Ketamine (100 mg/kg) and Xylazine (10 mg/kg) or Pentobarbital (40mg/kg) with inhalation of isoflurane in oxygen for maintenance. With 5 mm incision, the medial cortex of proximal tibia was exposed, then a hole was drilled in medial cortex with a 23G needle (0.65 mm in diameter) without penetrating the lateral cortex; then the lateral cortex was drilled through the medial hole with a 30G needle (0.3 mm diameter). The L-shaped implant which was inoculated bacteria or vehicle was inserted from the medial side and press-fit with its long end and its L tightly pressed against the medial side of the tibia. The initial bacterial burden determined from Colony forming unit (CFU) assay from the implant just before the insertion was 0.00 in Sterile, 1.6×10^5 in RP62A and 2.1×10^5 in USA300. The bacterial load of *S.epidermidis* was sufficient to cause toxicity from a previous report-results[23]. After surgery, mice were returned to standard isolator cages without additional treatment until sacrifice at day 14 unless otherwise described, and buprenorphine was administrated for their pain relief for 2 days.

Overview and sample size of experiments

To know the bacterial survival and bacterial burden in the tissue and on the implant, CFU assay was used (n=10 in each group). To know the difference of host reaction against different pathogens, histopathological and morphological (micro-computed tomography (μCT)) experiments were performed, and to know the biofilm formation which possibly related to the inhibition of osseous integration, implant was analyzed using scanning electron microscopy (SEM) with quantitative measurement (n=5 in each group). To know the host reaction in transcriptome, mRNA expression was evaluated using quantitative real-time PCR (qPCR) (n=4 in each group). For above mentioned experiments, sample size was determined according to the previous experiments [21,24–27]. Finally and most importantly, actual implant loosening was evaluated using biomechanical pushout test. The sample size of was estimated by preliminary experiment in rat (unpublished data). According to the data, to obtain 10 N difference, with standard deviation of 7 N, the calculated sample size was n = 8 under the condition of type I error was 0.05 and type II error was 0.80, then two extras were added and n = 10 in each group was determined.

All experiments were planned using 14 days samples. To confirm that all *S. epidermidis* samples established infection in earlier time point, 7 days experiments were added in CFU assay, and to confirm that small amount of S. epidermidis biofilm was at plateau and mature at 14 days, 42 days experiments were added, to deny the further growth of the biofilm. [21] The chart of the overview and sample size was showed in Fig. 1.

Ex vivo analysis

Bacterial survival in the tissue and on the implant using CFU analysis, as previously described. [21,24] Briefly, after euthanizing, implants were removed from tibiae gently using sterile forceps and the bone with surrounding soft tissue was weighed, minced and homogenized in PBS, and implant was sonicated and vortexed in PBS, then spread on TSB agar plate. CFU at 24 hours was calculated. To ensure if there were small colony variants, the cultures continued until day 14.

For image analyses, tibiae were harvested and fixed in 4% paraformaldehyde, then analyzed by high-resolution μCT (VivaCT 40; Scanco Medical AG, Basserdorf, Switzerland) to render three-dimensional images of the diaphysis as we have previously described. The maximal osteolytic area of medial and lateral cortex was measured for each specimen.

After μCT analysis, the tibiae were decalcified in EDTA and stained with alcian blue hematoxylin/orange G (ABH/OG) and Brown and Brenn to evaluate morphology, gram positive bacteria, and formation of *Staphylococcus* abscess communities (SAC), or with tartrate-resistant acid phosphatase (TRAP) to evaluate osteoclast as previously described.[24]

After the tibiae and fixed in 2.5% glutaraldehyde and 4% paraformaldehyde overnight, and then decalcified in 14% EDTA for 3 to 4 days, stainless steel implants were gently removed. The implants were post-fixed for 30 minutes in 1.0% osmium tetroxide in 0.1M Millonig's phosphate buffer, rinsed in distilled water, dehydrated through a graded series of ethanol to 100%, and sputter coated with gold for photography using a Zeiss Auriga Field Emission SEM. To measure area of the biofilm, pictures of the 1 mm^2 region of interest were cropped

and converted pixel-by-pixel to either green (whiter area than stainless steel surface) or blue (blacker area), then to obtain binary data, both green and blue area were converted to black (stainless surface) and other area to white (biofilm) using ImageJ (NIH, Bethesda, MD). Percent biofilm area was defined using this formula: %biofilm area = tissue area (white) / total area (black plus white).[21] Although there should be no bacterial biofilm on the implant, a small amount of host tissues are found on the sterile implant. The area of the tissues on the implant was also defined as %biofilm area for descriptive purpose. [21]

PCR analysis

For gene expression studies, tibiae were frozen in liquid nitrogen and crushed. Total RNA was extracted directly from harvested tibiae with TriPure Isolation Reagent (SIGMA-ALDRICH, Cat No 16757). Next, reverse transcribed with ReverTra Ace qPCR Master Mix (Toyobo, Japan). Finally, RT-qPCR was carried out on the Step One Plus (Applied Biosystems) with Thunderbird SYBR qPCR Mix (Toyobo). The analyzed transcriptomes are listed below; tumor necrosis factor-α (*TNF-α)*, Interleukin-1 *beta* (IL-1β), Interleukin-6 (IL-6), toll like receptor 2 (Tlr2), receptor activator for nuclear factor-κB ligand (RANKL), receptor activator of nuclear factor κB (RANK), dendrocyte expressed seven transmembrane protein (DC-STAMP), Cathepsin K (CTSK), Runt-related transcription factor 2 (Runx2), Osterix (Osx), *Alkaline Phosphatase* (ALP), Osteocalcin (Ocn) and collagen type I alpha 1 chain (Col1a1). The expression of genes was normalized to β-actin expression, expressed as 2-(ΔCt). Detailed information of the primers is provided as Supplement Table 1.

Biomechanical test

A biomechanical push-out test was used to quantify the strength of bonding of the implant to the tibiae. The same transtibial infection model was used with a modified implant, which was cut to 10 mm length and bent into an L-shaped implant: long side 9 mm, short side 1 mm. After sacrifice at day 14, the soft tissues around the implant were gently removed not to damage the tibia and implant. Each tibia with implant was rigidly immobilized with vise clamp to allow loading longitudinal-axes force to wire using a flat tip metal. The protruding implant was pushed from the lateral edge using an Instron-type testing machine (MZ-500S, Maruto Instrument Co. Ltd., Tokyo, Japan). The vertical force was applied on the edge of the implant with the speed of 1 mm per 1 minutes, and the maximum load during pushing was recorded.[28]

Statistical analyses.

To determine the incidence of infected implants and surrounding tissues based on CFUs, significant differences between groups were determined by Fisher's exact test. The comparison of bacterial burden in CFU, hole size in μCT, %Biofilm area in SEM, relative gene expression in qPCR, and push-out force were performed with exact Wilcoxon test with adaptive Hochberg multiplicity adjustment was used. Differences in which $p < 0.05$ were considered significant.

Results

In this surgical model, infection was limited locally in all mice and physical debilitation was not observed. There were no surgery related deaths in the experiments. As expected, no CFU were recovered from any of the tissue or implant samples in the Sterile group, and 100% of the tissues and implants in the USA300 group contained significant CFU (Fig. 2). Although RP62A achieved 100% infection of the tissue and 60% colonization of the implant on day 7, the bacterial burden was significantly less than that achieved by USA300 ($p < 0.001$, $p < 0.001$, respectively) by several orders of magnitude (Fig. 2A, B). Additionally, this pathogenic potential was significantly less than that of USA300 in bacterial load on day 14 (tissue; $p < 0.001$, implant; $p < 0.001$, respectively) (Fig. 2C, D) (Supplement Table 2).

As osteolysis and reactive bone formation are salient radiographic features of implant-associated osteomyelitis, we performed *ex vivo* μCT on challenged tibiae (Fig. 3). Gross analysis of tibiae challenged with Sterile implants revealed no signs of infection, and had the appearance of osseous integration. In contrast, USA300 challenged tibiae displayed massive osteolysis around the implant, and extensive reactive bone formation on the cortical surface. Remarkably, RP62A challenged tibiae were indistinguishable from the Sterile implant controls in μCT. These observations were confirmed via quantitative analysis of the implant hole-size, which showed the USA300 group had larger holes versus both the Sterile group and the RP62A group, on both the medial (1.79 ± 0.31 mm^2) and lateral (0.99 ± 0.32 mm^2) sides (Fig. 3B). Of note, the hole sizes of the Sterile group (medial: 0.15 ± 0.10 mm^2, lateral 0.08 ± 0.04 mm^2) and the RP62A challenged group (medial: 0.19 ± 0.14 mm^2, lateral 0.09 ± 0.05 mm^2) were close to the cross sectional area of the implant (0.10 mm^2).

To carefully assess differences in histopathology, and confirm our observations of infection, osteolysis, and implant osseous integration, we performed histology on the tibiae from the three groups (Fig. 4). Alcian blue-hematoxylin/orange G (ABH/OG) staining failed to demonstrate any remarkable histopathology in the RP62A challenged tibiae compared to the Sterile controls, as there was copious bone new bone formation around the implant, intact cortical bone, and normal bone marrow throughout (Fig 4A, B). In contrast, the marrow was destroyed in USA300 infected tibiae (Fig. 4C) and was replaced by *Staphylococcus* abscess communities (SACs). Brown and Brenn staining confirmed the absence of Gram-positive bacteria in both the Sterile implant and RP62A infected groups (Fig. 4D, E). However, Gram-positive clusters of bacteria could be readily seen in the center of the SACs within USA300 infected tibiae and the surrounding soft tissues (Fig. 4F). Interestingly, staining for tartrate-resistant acid phosphatase (TRAP) revealed more osteoclasts remodeling the new bone formed around the implant in the RP62A group versus the Sterile group (Fig. 4G, H). Moreover, the high-power micrographs revealed contiguous new bone formation completely around the implants in the Sterile group (Fig. 4D, G), while the new bone formation around the RP62A infected implants was incomplete and contained fibrous tissue at the host-implant interface in all specimens (Fig. 4E, H). TRAP staining of USA300 infected tibiae confirmed the presence of large numbers of osteoclasts at sites of cortical bone erosion and remodeling reactive bone (Fig. 4I).

To assess biofilm formation on the implants 14 and 42-days post-op, we performed a region of interest (ROI) quantitative SEM analysis of the explants (Fig. 5A, B). The results confirmed significant biofilm formation in the USA300 group compared to the Sterile and RP62A groups. Specifically, the percent biofilm area of the USA300 group (39.0 ± 13.7 %) was significantly larger than the Sterile (6.3 ± 2.3 %; $p = 0.03$) and RP62A (12.9 ± 7.4 %; $p = 0.03$) groups on day 14. Moreover, there was no significant difference in biofilm formation between RP62A infected and Sterile implants at this time point ($p = 0.18$). To assess whether this difference was owing to the slow growth of RP62A biofilm, we determined the percent biofilm area on day 42 post-op, which produced the same results. At this late time point, the % biofilm area of USA300 (37.7 ± 10.2 %) was still significantly larger than that of the Sterile (5.7 ± 4.3 %; $p = 0.03$) and RP62A (10.5 ± 3.1 %; $p = 0.03$) groups. Interestingly, the amount of biofilm formed on the RP62A infected implants was equivalent to the host material (cells and plasma proteins) adhered to Sterile implants, as determined by this ROI assay.

To confirm the absence of bacteria on the Sterile implants, and their presence in the biofilm on the RP62A and USA300 infected implants, we performed rigorous SEM assessments of the explants (Fig. 5C). While no bacteria were found on Sterile implants, a small number of cocci appeared together with the host components (i.e. fibrin) on both RP62A and USA300 infected implants. Additionally, this biofilm also contained empty lacunae, which is evidence of extravasated bacteria from mature biofilm.[21]

To assess inflammation, bone resorption and bone formation, qRT-PCR analyses were performed on the three groups of implanted tibiae. USA300 and RP62A infection significantly induced an inflammatory transcriptome, as IL-1β, IL-6 and Tlr2 mRNA levels were significantly increased compared to Sterile controls (Fig. 6). The infected tibiae also had significantly increased RANKL levels, consistent with inflammation-induce osteoclastogenesis, and the large numbers of TRAP+ cells observed in the histology. Consistent with the osteolysis observed in USA300-infected tibiae, gene expression for mature osteoclasts (CTSK) was increased, and bone formation gene expression (Col1a1) was decreased, versus Sterile implant and RP62A challenged tibiae.

To assess the effects of RP62A infection on osseous integration of the implants in our transtibial model, we performed biomechanical push-out testing on the three groups (Fig. 7). The results demonstrated osseous integration in the Sterile group, as remarkable force to push out the implants (17.3 ± 4.1 N), versus complete lack of bone integration in the USA300 group, as minimal forces (0.68 ± 0.30 N) was required to remove the implants, as expected based on the extensive osteolysis revealed by histology and μCT. Interestingly and importantly, RP62A infected implants required significantly greater force (7.5 ± 3.4 N) to remove from tibiae compared with the USA300 group ($p < 0.001$). However, the force to push-out RP62A infected implant was also significantly less than that in the Sterile group ($p < 0.001$), suggesting incomplete osseous integration as predicted by the histology and SEM analyses.

Discussions

Loosening of implants is still major clinical problems in implant associated orthopaedic infections[29]. Although *S. epidermidis* is commonly found on septic and aseptic loose orthopaedic implants, its pathogenic role in bone infection has been debated, since it is a constituent of healthy human microbiota, and participates in mutualistic symbiosis with the host in this capacity[30,31]. Thus, we aimed to directly test the pathogenic potential of *S. epidermidis* compared to highly virulent *S. aureus* using an established murine implant-associated osteomyelitis model. Here we demonstrated the specific features of RP62A infection during the process of implant-associated osteomyelitis. In contrast to USA300, which caused severe inflammation, complete marrow necrosis, extensive bone destruction, and abundant biofilm on the implant, RP62A failed to induce any gross pathology. Furthermore, RP62A formed an unquantifiable amount of biofilm on the implant, and collectively appeared as a silent infection in this model. However, RP62A infection showed elevated gene expression related to inflammation and osteoclastogenesis, and most importantly caused significant implant loosening.

A primary outcome measure of virulence is bacterial load in infected tissue. Thus, our finding of significant CFUs in tissues and on the implants of RP62A infected tibiae at 7-day and 14-day, formally establishes its pathogenesis in this murine model. However, *S. epidermidis* virulence is clearly limited compared to *S. aureus* infections, particularly in terms of its ability to establish osteomyelitis at 14-days, as six out of ten tissues, and four out of ten RP62A contaminated implants failed to culture out CFUs at 14 days. This finding is consistent with the results of Bart et al. who demonstrated that *S. aureus* colonization is greater than *S. epidermidis* on metal implants up to 48 hours, although the initial bacterial burden is equivalent [32].

Histologically, we observed drastic difference between USA300 and RP62A. While evidence of new bone formation around the implant was seen in both Sterile and RP62A groups, USA300 infected tibiae were destroyed from osteolysis, and new bone formation was restricted to periosteal apposition. *Staphylococcus* abscess communities (SACs) were also present throughout the bone marrow space and soft tissues in USA300- infected tibiae but were never observed in RP62A-challenged tibiae. This was expected, as *S. epidermidis* lacks coagulase and a von Willebrand factor-binding protein (clumping factor A), which are required for SAC formation [33]. As such, it is likely that interstitial *S. epidermidis* is rapidly cleared by host immune cells and fails to establish an infectious nidus in bone marrow or in the adjacent soft tissues. Consistently, we found no gram-positive bacterial clusters in RP62A challenged tibiae, although this diagnostic approach is known to have an 82% of negative predictive value for periprosthetic infection.[34] In contrast, histopathologic evidence of RP62A infection was apparent from large numbers of TRAP positive cells in remodeling bone and fibrous tissue around the implant compared to the Sterile group (Fig. 4 G&H). This is somewhat surprising considering no differences in μCT data were observed between the Sterile and RP62A groups (Fig. 3). However, this is consistent with the absence of clinical radiographic findings associated with *S. epidermidis* implant-associated bone infections,[35] and aseptic loosening of total joint replacements.[12,13] These observations are also consistent

with the findings of Lankinen et al, who demonstrated similar bone destruction tendencies to our results with a rabbit model.[36]

On SEM analysis, RP62A produced less biofilm compared to USA300. This was not due to slow biofilm formation, as there was no increase of %biofilm area between day 14 and 42, and the empty lacunae similar to that observed in mature USA300 biofilm[21] were already seen in RP62A infection at day 14 (Fig. 5C). Thus, similar to the histology results, the findings confirm a pathogenesis of RP62A, whose virulence is markedly limited from that of USA300 due to the absence of genes whose immune evasion functions usurp host factors to create a protective glycocalyx on the implant. Nonetheless, the limited RP62A-biofilm on the implant cannot be removed by the host, and likely inhibits osseous integration of orthopaedic implants.

Another surprising finding in our study was that RP62A stimulates a robust pro-inflammatory transcriptome, similar to that of USA300 (Fig.6), despite the absence of inflammatory cells and bone marrow destruction. While similar gene expression findings have been reported for *S. aureus* infections,[37,38] and *S. epidermidis in vitro* and *in vivo* studies,[39,40] the lack of osteolysis in this osteoclastogenic environment remains largely unexplained and remains an important future research direction.

Finally, implant loosening was observed in USA300 and RP62A implants, although the severity of the loosening was very different (Fig. 7). USA300 completely inhibited osseous integration, which is consistent with the extensive osteolysis observed in our histological and μCT analyses. By contrast, RP62A permitted some osseous integration, but also induced fibrotic tissue formation around the implant compared to Sterile controls. Of note is that similar histology and biomechanical testing results have been reported in clinical implant-associated *S. epidermidis* infections[41]. Thus, we believe this experimental model has excellent construct and face validity with the clinical orthopaedic problems caused by *S. epidermidis*, most notably, implant loosening.

There are several limitations in this study. First, we did not evaluate non-biofilm producing *S.epidermidis* strains, which may yield different results[9]. Second, we used CFU assays as our only outcome measure of infection, which is common in this field of research, although confirmatory molecular analyses such as bacterial gene PCR or next generation sequencing might be beneficial. Third, the distinction between *S. epidermidis* infection and colonization remains unclear in the absence of Gram positive histology. However, because of the clear evidence of histologic and biomechanical implant loosening, we believe the current results formally demonstrate RP62A's ability to cause infection in healthy animals. Nevertheless, further studies are warranted to distinguish minor acute infection from colonization and chronic infection, or from aseptic loosening. Fourth, our finding of the RP62A induced pro-inflammatory transcriptome in the absence of osteolysis remains unexplained. Thus, follow up studies to investigate negative feedback gene expression (e.g. soluble (IL1-receptor antagonist and osteoprotegrin) and intracellular (suppressors of cytokine signaling (SOCSs)) are needed. Additionally, studies designed to determine if the induced transcriptome is caused directly by *S. epidermidis,* or implant micromotion are also critical for establishing the root cause of the clinical problem. Finally, we did not investigate implant loosening after

a long-term follow-up; only SEM was observed at 42 days. This is important, as the differential diagnosis between clinical aseptic loosening and *S. epidermidis* infection can only be established after long-term follow-up from the initial surgery. Furthermore, recent reports describe that more than half of the implant removed from healthy patients were culture or PCR positive for *S. epidermidis*.[42]

In summary, we found biofilm-producing RP62A is incapable of directly inducing the prominent pathological features of implant-associated osteomyelitis, including osteolysis, reactive bone formation and marrow ablation. However, RP62A can be considered pathogenic in orthopaedic settings, as it can persist in biofilm on the implant, and stimulates a pro-inflammatory environment and incomplete osseous integration of the implant. Thus, these results support a role for RP62A in implant loosening, as the bacteria can form small amounts of biofilm that inhibit osseous integration and bone healing. Therefore, RP62A should be considered as a low-grade pathogen of osteomyelitis, especially in implant associated cases and asymptomatic implant loosening.

Supplementary Material

Refer to Web version on PubMed Central for supplementary material.

ACKNOWLEDGMENTS

The authors would like to thank Drs. Paul Dunman and Steven Gill for providing us with several *Staphylococci* strains, Gayle Schneider for technical assistance with the electron microscopy sample preparations. We also show gratitude Keiko Furuta and Haruyasu Kohda for practical support in electron microscopy. This study was supported by Grant-in-Aid for Research Activity start-up (16H06906), ISHIZUE 2017 of Kyoto University Research Development Program, 2017 Research grant of Fujiwara Memorial Foundation, this study was also supported by NIAMS/NIH grants P30AR069655 and P50AR072000, and the AOTrauma Clinical Priority Program.

REFERENCES

1. Schwarz EM, Parvizi J, Gehrke T, et al. 2019 2018 International Consensus Meeting on Musculoskeletal Infection: Research Priorities from the General Assembly Questions. J. Orthop. Res. 37(5):997–1006 [PubMed: 30977537]
2. Saeed K, McLaren AC, Schwarz EM, et al. 2019 2018 international consensus meeting on musculoskeletal infection: Summary from the biofilm workgroup and consensus on biofilm related musculoskeletal infections. J. Orthop. Res. 37(5):1007–1017. [PubMed: 30667567]
3. Goetz C, Tremblay YDN, Lamarche D, et al. 2017 Coagulase-negative staphylococci species affect biofilm formation of other coagulase-negative and coagulase-positive staphylococci. J. Dairy Sci. 100(8):6454–6464. [PubMed: 28624271]
4. Kourbatova EV., Halvosa JS, King MD, et al. 2005 Emergence of community-associated methicillin-resistant Staphylococcus aureus USA 300 clone as a cause of health care-associated infections among patients with prosthetic joint infections. Am. J. Infect. Control 33(7):385–391. [PubMed: 16153484]
5. Teterycz D, Ferry T, Lew D, et al. 2010 Outcome of orthopedic implant infections due to different staphylococci. Int. J. Infect. Dis. 14(10):e913–e918. [PubMed: 20729115]
6. Bradbury T, Fehring TK, Taunton M, et al. 2009 The Fate of Acute Methicillin-Resistant Staphylococcus aureus Periprosthetic Knee Infections Treated by Open Debridement and Retention of Components. J. Arthroplasty 24(6 SUPPL):101–104.
7. Bassetti M, Trecarichi EMM, Mesini A, et al. 2012 Risk factors and mortality of healthcare-associated and community-acquired Staphylococcus aureus bacteraemia. Clin. Microbiol. Infect. 18(9):862–869. [PubMed: 21999245]

8. Nixon M, Jackson B, Varghese P, et al. 2006 Methicillin-resistant Staphylococcus aureus on orthopaedic wards. J. Bone Joint Surg. Br. 88-B(6):812–817. [PubMed: 16720779]
9. Otto M 2009 Staphylococcus epidermidis — the “accidental” pathogen. Nat. Rev. Microbiol. 7(8):555–567. [PubMed: 19609257]
10. Iwase T, Uehara Y, Shinji H, et al. 2010 Staphylococcus epidermidis Esp inhibits Staphylococcus aureus biofilm formation and nasal colonization. Nature 465(7296):346–349. [PubMed: 20485435]
11. Vuong C, Otto M. 2002 Staphylococcus epidermidis infections. Microbes Infect. 4(4):481–9. [PubMed: 11932199]
12. Jacobs AME, Bénard M, Meis JF, et al. 2017 The unsuspected prosthetic joint infection. Bone Joint J. 99-B(11):1482–1489. [PubMed: 29092987]
13. Nelson CL, McLaren AC, McLaren SG, et al. 2005 Is aseptic loosening truly aseptic? Clin. Orthop. Relat. Res. NA;(437):25–30.
14. Ettinger M, Calliess T, Kielstein JT, et al. 2015 Circulating Biomarkers for Discrimination between Aseptic Joint Failure, Low-Grade Infection, and High-Grade Septic Failure. Clin. Infect. Dis. 61(3):332–341. [PubMed: 25870326]
15. Bogut A, Niedzwiadek J, Koziol-Montewka M, et al. 2014 Characterization of Staphylococcus epidermidis and Staphyloccocus warneri small-colony variants associated with prosthetic-joint infections. J. Med. Microbiol. 63(Pt_2):176–85. [PubMed: 24257683]
16. Trampuz A, Piper KE, Jacobson MJ, et al. 2007 Sonication of Removed Hip and Knee Prostheses for Diagnosis of Infection. N. Engl. J. Med. 357(7):654–663. [PubMed: 17699815]
17. Boot W, Moojen DJF, Visser E, et al. 2015 Missed low-grade infection in suspected aseptic loosening has no consequences for the survival of total hip arthroplasty Missed low-grade infection in suspected aseptic loosening has no consequences for the survival of total hip arthroplasty.3674.
18. Hoenders CSM, Harmsen MC, Van Luyn MJA. 2008 The local inflammatory environment and microorganisms in “aseptic” loosening of hip prostheses. J. Biomed. Mater. Res. - Part B Appl. Biomater. 86(1):291–301. [PubMed: 18098200]
19. Sugimoto S, Iwamoto T, Takada K, et al. 2013 Staphylococcus epidermidis Esp Degrades Specific Proteins Associated with Staphylococcus aureus Biofilm Formation and Host-Pathogen Interaction. J. Bacteriol. 195(8):1645–1655. [PubMed: 23316041]
20. Gill SR, Fouts DE, Archer GL, et al. 2005 Insights on Evolution of Virulence and Resistance from the Complete Genome Analysis of an Early Methicillin-Resistant. Society 187(7):2426–2438.
21. Nishitani K, Sutipornpalangkul W, de Mesy Bentley KL, et al. 2015 Quantifying the natural history of biofilm formation in vivo during the establishment of chronic implant-associated Staphylococcus aureus osteomyelitis in mice to identify critical pathogen and host factors. J. Orthop. Res. 33(9):1311–1319 Available from: http://doi.wiley.com/10.1002/jor.22907. [PubMed: 25820925]
22. Fey PD, Endres JL, Yajjala VK, et al. 2013 A genetic resource for rapid and comprehensive phenotype screening of nonessential Staphylococcus aureus genes. MBio 4(1):e00537–12. [PubMed: 23404398]
23. Goëau-Brissonnière O, Mercier F, Nicolas MH, et al. 1994 Treatment of vascular graft infection by in situ replacement with a rifampin-bonded gelatin-sealed Dacron graft. J. Vasc. Surg. 19(4):739–744. [PubMed: 8164289]
24. Varrone JJ, de Mesy Bentley KL, Bello-Irizarry SN, et al. 2014 Passive immunization with anti-glucosaminidase monoclonal antibodies protects mice from implant-associated osteomyelitis by mediating opsonophagocytosis of Staphylococcus aureus megaclusters. J. Orthop. Res. 32(10):1389–1396. [PubMed: 24992290]
25. Farnsworth CW, Schott EM, Benvie AM, et al. 2018 Obesity/type 2 diabetes increases inflammation, periosteal reactive bone formation, and osteolysis during Staphylococcus aureus implant-associated bone infection. J. Orthop. Res. 36(6):1614–1623. [PubMed: 29227579]
26. Inzana JA, Schwarz EM, Kates SL, Awad HA. 2015 A novel murine model of established Staphylococcal bone infection in the presence of a fracture fixation plate to study therapies utilizing antibiotic-laden spacers after revision surgery. Bone 72:128–136. [PubMed: 25459073]

27. Takahata M, Schwarz EM, Chen T, et al. 2012 Delayed short-course treatment with teriparatide (PTH1–34) improves femoral allograft healing by enhancing intramembranous bone formation at the graft-host junction. J. Bone Miner. Res. 27(1):26–37. [PubMed: 21956542]
28. Giavaresi G, Fini M, Cigada A, et al. 2003 Mechanical and histomorphometric evaluations of titanium implants with different surface treatments inserted in sheep cortical bone. Biomaterials 24(9):1583–1594. [PubMed: 12559818]
29. Worlock P, Slack R, Harvey L, Mawhinney R. 1994 The prevention of infection in open fractures: an experimental study of the effect of fracture stability. Injury 25(1):31–38. [PubMed: 8132308]
30. Pajarinen J, Cenni E, Savarino L, et al. 2010 Profile of toll-like receptor-positive cells in septic and aseptic loosening of total hip arthroplasty implants. J. Biomed. Mater. Res. - Part A 94(1):84–92.
31. Huttenhower C, Gevers D, Knight R, et al. 2012 Structure, function and diversity of the healthy human microbiome. Nature 486(7402):207–214. [PubMed: 22699609]
32. Barth Elin, Quentin M, Myrvik et al. 1989 In vitro and in vivo comparative colonization of Staphylococcus aureus and Staphylococcus epidermidis on orthopaedic implant materials. Biomaterials 10(5):325–328. [PubMed: 2765629]
33. Cheng AG, McAdow M, Kim HK, et al. 2010 Contribution of Coagulases towards Staphylococcus aureus Disease and Protective Immunity. PLoS Pathog. 6(8):19–20.
34. Della Valle CJ, Scher DM, Kim YH, et al. 1999 The role of intraoperative gram stain in revision total joint arthroplasty. J. Arthroplasty 14(4):500–504. [PubMed: 10428233]
35. Trampuz A, Zimmerli W. 2005 Prosthetic joint infections: Update in diagnosis and treatment. Swiss Med. Wkly. 135(17–18):243–251. [PubMed: 15965826]
36. Lankinen P, Lehtimäki K, Hakanen AJ, et al. 2012 A comparative 18F-FDG PET/CT imaging of experimental Staphylococcus aureus osteomyelitis and Staphylococcus epidermidis foreign-body-associated infection in the rabbit tibia. EJNMMI Res. 2(1):1–10. [PubMed: 22251281]
37. Kassem A, Lindholm C, Lerner UH. 2016 Toll-Like receptor 2 stimulation of osteoblasts mediates staphylococcus aureus induced bone resorption and osteoclastogenesis through enhanced RANKL. PLoS One 11(6):1–20.
38. Cao F, Zhou W, Liu G, et al. 2017 Staphylococcus aureus peptidoglycan promotes osteoclastogenesis via TLR2-mediated activation of the NF-κB/nfatc1 signaling pathway. Am. J. Transl. Res. 9(11):5022–5030. [PubMed: 29218100]
39. Laborel-Préneron E, Bianchi P, Boralevi F, et al. 2015 Effects of the Staphylococcus aureus and Staphylococcus epidermidis Secretomes Isolated from the Skin Microbiota of Atopic Children on CD4+ T Cell Activation. PLoS One 10(10):e0141067. [PubMed: 26510097]
40. Svensson S, Trobos M, Omar O, Thomsen P. 2017 Site-specific gene expression analysis of implant-near cells in a soft tissue infection model - Application of laser microdissection to study biomaterial-associated infection. J. Biomed. Mater. Res. Part A 105(8):2210–2217.
41. Veiranto NAM, Tiainen ESJ, Niemel S. 2006 Innovation in multifunctional bioabsorbable osteoconductive drug-releasing hard tissue fixation devices.:1275–1282.
42. Knabl L, Kuppelwieser B, Mayr A, et al. 2019 High percentage of microbial colonization of osteosynthesis material in clinically unremarkable patients. Microbiologyopen 8(3):e00658. [PubMed: 30508282]

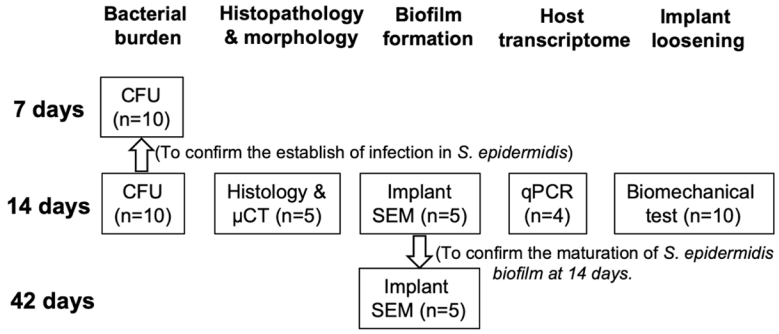

Figure 1. Flow chart of each experiments.

CFU = colony forming unit, µCT = micro-computed tomography, SEM = scanning electron microscopy, qPCR = quantitative polymerase chain reaction

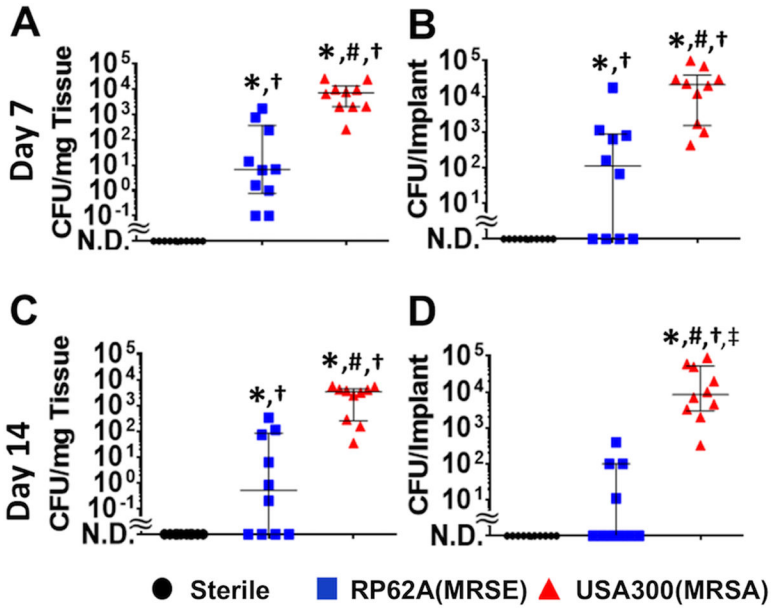

Figure 2. Decreased incidence and bacterial burden of RP62A implant-associated osteomyelitis compared to USA300.

Mice were challenged with a transtibial implant containing no bacteria (Sterile), 1.6×10^5 CFU of RP62A, or 2.1×10^5 CFU of USA300, and euthanized on day 7 (A, B), or day 14 (C, D) post-op. The challenged tissues (A, C) and implants (B, D) were harvested and processed for CFU content, and the data are presented for each mouse in the group (n=10) with median and interquartile range (N.D.=not detectable; *p<0.05 vs. Sterile, #p<0.05 vs. RP62A). Statistical assessment of the incidence of CFU are shown (†p<0.05 vs. Sterile, ‡p<0.05 vs. RP62A).

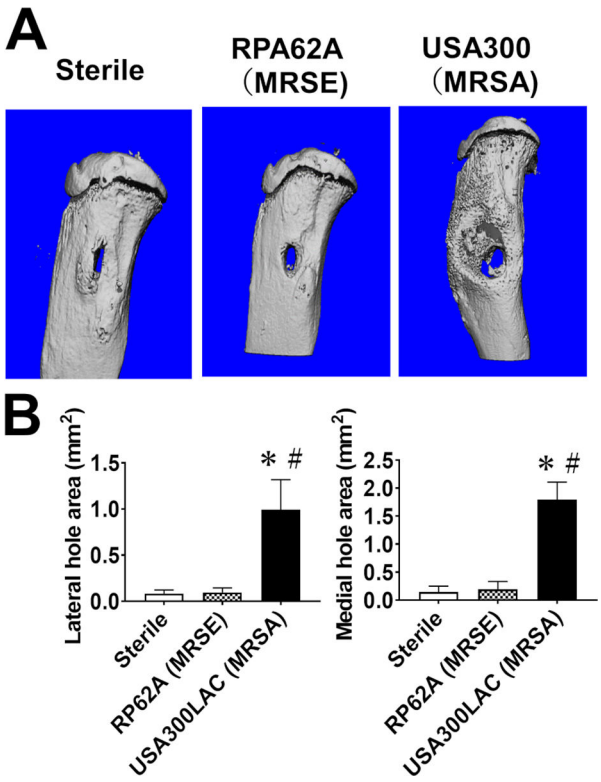

Figure 3. Absence of osteolysis and reactive bone formation in RP62A infected tibiae.

Mice (n=5) were challenged with a transtibial implant containing no bacteria (Sterile), 1.6×10^5 CFU of RP62A, or 2.1×10^5 CFU of USA300, euthanized on day 14 post-op, and the challenged tibiae were analyzed by micro-CT. (A) Representative 3D renderings of a tibia from each group are shown to illustrate the remarkable osteolysis and reactive bone formation in USA300 infected tibiae, versus the osseous integrated Sterile implant. Of note is that the RP62A infected tibiae were grossly indistinguishable from the Sterile implant group. (B) The lateral and medial hole area of the challenged tibiae were determined from the micro-CT scans, and the means ± SD are presented (*$p<0.05$ vs. Sterile; #$p<0.05$ vs. RP62A).

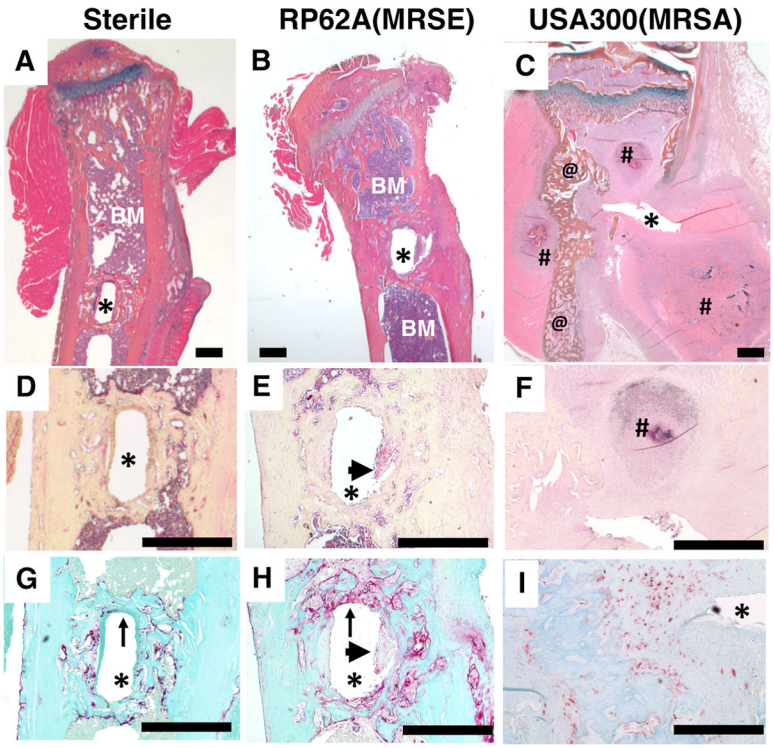

Figure 4. Absence of histopathology in RP62A infected tibiae.

The tibias described in Figure 3 were processed for demineralized histology and representative micrographs of sections stained with Alcian blue hematoxylin/orange G (A-C), Brown and Brenn (D-F) and tartrate-resistant acid phosphatase (TRAP) (G-I) are shown at 25x (A-C) and 50x (D-I) (bar = 0.5mm). The implant insertion site is indicated by the asterix (*). Note the presence of normal bone marrow (BM) flanking the new bone that formed around the implant in the RP62A infected tibia, in contrast to the *S. aureus* infected tibia in which the marrow has been destroy and replaced by Staphylococcus abscess communities (#). The massive osteolysis and reactive bone formation (@) observed in USA300 infected tibiae via micro-CT was confirmed by histology (C). Although no gross pathology (B) or Gram positive bacteria staining (E) was detected in RP62A infected tibia, a lack of complete implant osseous integration was apparent from discontinuous bone formation around the implant (arrows in G vs. H), and fibrous tissue at the host-implant interface (arrowheads in E & H).

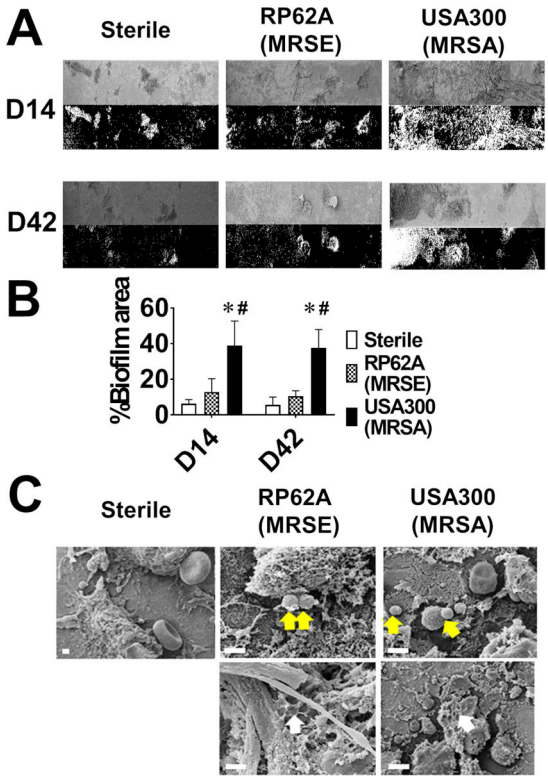

Figure 5. Lack of biofilm on explants from RP62A infected tibiae.

Mice (n=5) were challenged with a transtibial implant containing no bacteria (Sterile), 1.6×10^5 CFU of RP62A, or 2.1×10^5 CFU of USA300, euthanized on day 14 or 42 post-op, and the implants were process for scanning electron microscopy (SEM) to assess biofilm formation. (A) Representative SEM images of the region of interest (ROI) at x100 (top panel) are shown with the ImageJ rendering of the biofilm (lower panel), to illustrate the similarity between the Sterile and RP62A groups, in contrast to the great amount of biofilm formed on the USA300 infected implants. (B) The % of ROI surface area covered with biofilm was quantified with ImageJ, and the data are presented as the mean ± SD (*$p<0.05$ vs. Sterile; #$p<0.05$ vs. RP62A). Of note is that there were no significant differences between the Sterile and RP62A groups, or day 14 vs. 42. (C) High power SEM images are shown at x5,000 in Sterile and x15,000 in RP62A and USA300 to illustrate that the only matter observed on Sterile implants was red blood cells and host material. In contrast, cocci (yellow arrows) and empty lacunae (white arrows) were present in RP62A and USA300 biofilm.

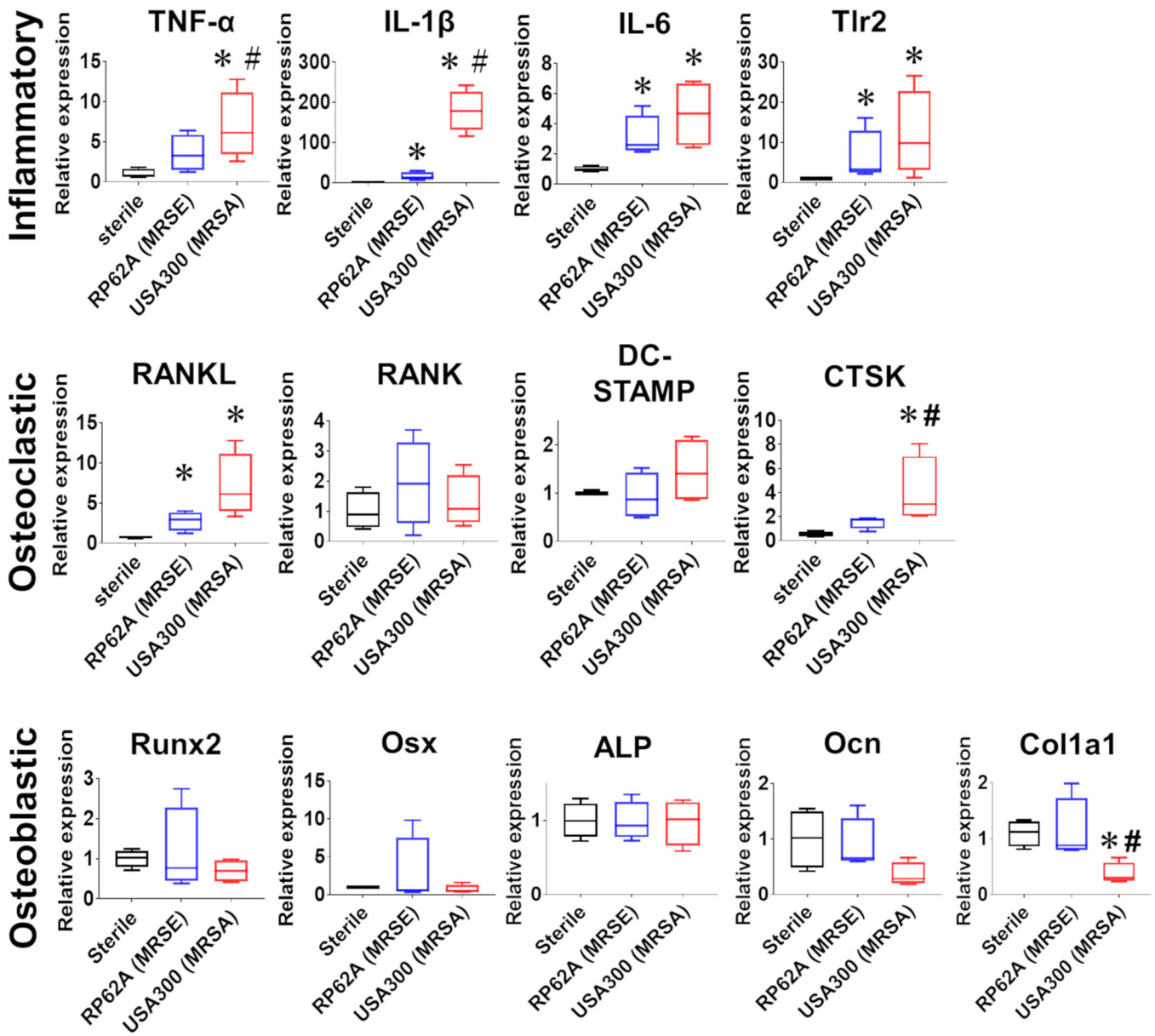

Figure 6. Proinflammatory transcriptome in RP62A infected tibiae.

Mice (n=4) were challenged with a transtibial implant containing no bacteria (Sterile), 1.6×10^5 CFU of RP62A, or 2.1×10^5 CFU of USA300, euthanized on day 14, and their tibiae were process for qPCR. Relative gene expression data are presented as the fold change from Sterile control with the mean ± SD (*$p < 0.05$ vs. Sterile, ♯$p < 0.05$ vs *S.epidermidis*). Of note is that there were no significant differences between *S. epidermidis* and *S. aureus*, and no differences between groups in most osteoblastic gene expression.

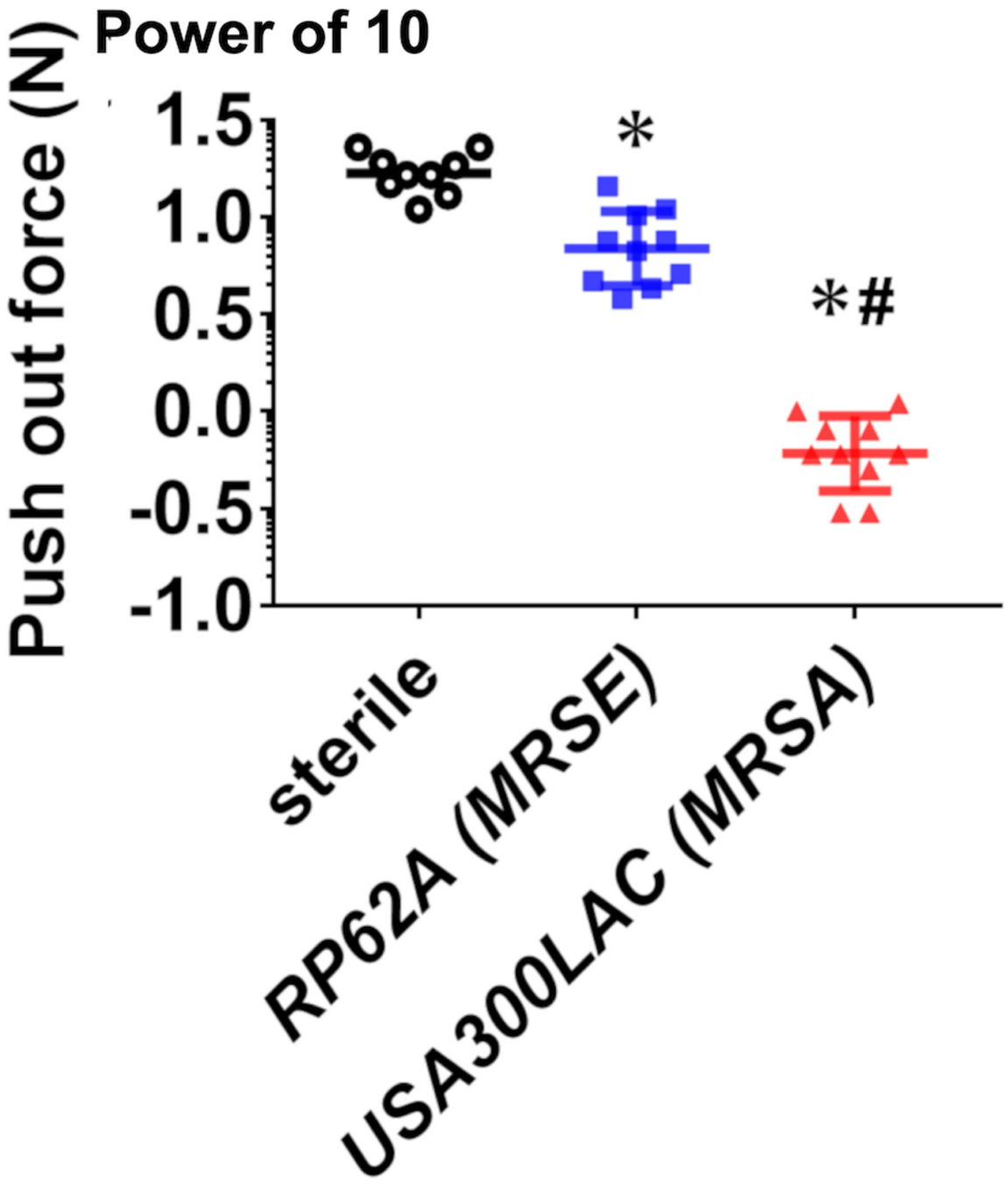

Figure 7. Limited osseous integration of transtibial implants into *S. epidermidis* infected tibiae.
Mice (n=10) were challenged with a transtibial implant containing no bacteria (Sterile), 1.6×10^5 CFU of RP62A, or 2.1×10^5 CFU of USA300, euthanized on day 14, and their tibiae were harvested for biomechanical put out testing. The data for each tibia is presented with the mean for the group ± SD (*$p < 0.001$ vs. Sterile; #$p < 0.001$ vs. RP62A). Of note is that there were significant differences between Sterile and RP62A, and RP62A and USA300.